

# Template Control over Dimerization and Guest Selectivity of Interpenetrated Coordination Cages

Sabrina Freye,<sup>†</sup> Reent Michel,<sup>†</sup> Dietmar Stalke,<sup>†</sup> Martin Pawliczek,<sup>‡</sup> Holm Frauendorf,<sup>‡</sup> and Guido H. Clever<sup>\*†</sup>

<sup>†</sup>Institute for Inorganic Chemistry, Georg-August-Universität Göttingen, Tammannstraße 4, 37077 Göttingen, Germany

<sup>‡</sup>Institute for Organic and Biomolecular Chemistry, Georg-August-Universität Göttingen, Tammannstraße 2, 37077 Göttingen, Germany

**S** Supporting Information

**ABSTRACT:** We have previously shown that the self-assembly of dibenzosuberone-based bis-monodentate pyridyl ligands  $L^1$  with  $Pd^{II}$  cations leads to the quantitative formation of interpenetrated coordination cages  $[BF_4@Pd_4L^1_8]$ . The  $BF_4^-$  anion inside the central cavity serves as a template, causing the outer two pockets to show a tremendous affinity for allosteric binding of two small chloride anions. Here we show that derivatization of the ligand backbone with a bulky aryl substituent allows us to control the dimerization and hence the guest-binding ability of the cage by the choice of the templating anion. Steric constraints imposed by  $L^2$  prevent the large  $BF_4^-$  anion from serving as a template for the formation of interpenetrated double cages. Instead, a single isomer of the monomeric cage  $[Pd_2L^2_4]$  is formed. Addition of the small anionic template  $Cl^-$  permits dimerization, yielding the interpenetrated double cage  $[Cl@Pd_4L^2_8]$ , whose enlarged outer pockets show a preference for the binding of large anions such as  $ReO_4^-$ .

Nanosopic rings and cages based on hydrogen-bonded<sup>1</sup> or metal-mediated<sup>2</sup> self-assembly are widely used as hosts for the encapsulation of guest species. Recent work by Fujita, Stang, Nitschke, and others has spurred the understanding of the assembly principles with respect to the size, shape, and guest-binding capabilities of such structures.<sup>3</sup> Anion binding by positively charged coordination cages has been applied in various sensing, transport, and separation tasks<sup>4</sup> and in the construction of functional supramolecular systems such as stacked metal arrays<sup>5</sup> and assemblies capable of light-triggered crystallization.<sup>6</sup> One prerequisite for the formation of such non-covalent assemblies is a large value of the host–guest association constant ( $K$ ).  $K$  is a function of the guest's charge (i.e., its charge density and distribution) and size.<sup>7</sup> The dependence on the latter parameter can be optimized by screening a series of homologous cage derivatives with the aim of finding the ideal match between the size of the anionic guest and the cavity.

To minimize the synthetic effort associated with the generation of such cage libraries, we envisioned two alternative strategies for the preparation of adjustable anion-binding systems:<sup>8</sup> one approach uses light-switchable cage structures to modulate the cavity size,<sup>9</sup> and the other method is based on

template control of the pocket sizes in interpenetrated<sup>10</sup> coordination cages. Toward the realization of the latter approach, we recently reported the anion-binding capabilities of a dimeric intercatenated coordination cage,  $[BF_4@Pd_4L^1_8]$ , containing one templating  $BF_4^-$  anion tightly bound in its central cavity and two loosely bound  $BF_4^-$  anions in the symmetry-equivalent outer pockets.<sup>11</sup> The outer two anions can be replaced by two halide anions in a positive cooperative-binding process (Figure 1a).<sup>12</sup> Chloride is bound with tremendous affinity ( $K_{net} \approx 10^{20} M^{-2}$ ), as exemplified by the cage's ability to dissolve  $AgCl$  in acetonitrile.<sup>13</sup> We further showed that the allosteric binding mechanism induces a shrinking of the double cage along the  $Pd_4$  axis by 3.3%, accompanied by a relative torsion of the two intercatenated

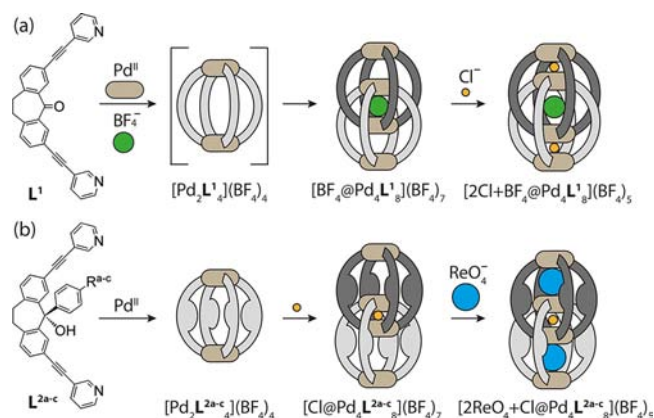


**Figure 1.** (a) The addition of  $[Pd(CH_3CN)_4](BF_4)_2$  to ligand  $L^1$  leads to the formation of the thermodynamically unstable monomeric cage  $[Pd_2L^1_4](BF_4)_4$ , which rearranges quantitatively to give the  $BF_4^-$ -templated, interpenetrated double cage  $[BF_4@Pd_4L^1_8](BF_4)_7$ . The latter is able to bind two chloride anions in its small outer pockets. (b) Addition of  $[Pd(CH_3CN)_4](BF_4)_2$  to ligands  $L^{2a-c}$  ( $R^a = CF_3$ ;  $R^b = OCH_3$ ;  $R^c = CH_3$ ) leads to the formation of the thermodynamically stable monomeric cages  $[Pd_2L^{2a-c}_4](BF_4)_4$ . Addition of 0.5 equiv of chloride then leads to the templated formation of the dimers  $[Cl@Pd_4L^{2a-c}_8](BF_4)_7$ . The latter can bind two perchlorate anions in their large outer pockets. All external and all loosely bound  $BF_4^-$  counter anions (inside the monomeric cages and the outer pockets of the dimeric cages) have been omitted for clarity.

Received: April 2, 2013

Published: May 22, 2013

{Pd<sub>2</sub>L<sub>4</sub>} units by 8<sup>o</sup>.<sup>13,14</sup> This mechanism poses the following question: Can the choice of the anion inside the central pocket be used to control the anion-binding selectivity in the outer two pockets via a structural relay effect?

To investigate this question, we synthesized the modified bimonodentate pyridyl ligands L<sup>2a-c</sup> (R<sup>a</sup> = CF<sub>3</sub>; R<sup>b</sup> = OCH<sub>3</sub>; R<sup>c</sup> = CH<sub>3</sub>) carrying a bulky aryl substituent attached to the ligand's central backbone carbonyl atom (Figure 1b) via Grignard additions to L<sup>1</sup>. When ligand L<sup>2a</sup> was treated with a stoichiometric amount of [Pd(CH<sub>3</sub>CN)<sub>4</sub>](BF<sub>4</sub>)<sub>2</sub> in acetonitrile, a single isomer of the monomeric coordination cage [Pd<sub>2</sub>L<sup>2a</sup>]<sub>4</sub> was formed quantitatively, as indicated by the shift (but not splitting) of the signal observed in the <sup>1</sup>H NMR spectrum [Figure 2a(i,ii)] and the occurrence of peaks for the species

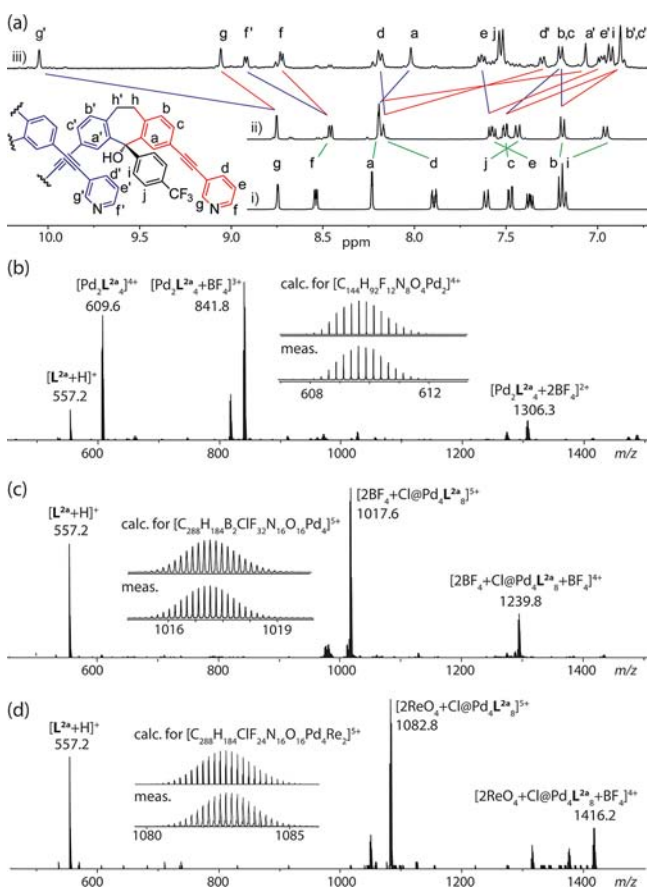


**Figure 2.** (a) <sup>1</sup>H NMR spectra of (i) ligand L<sup>2a</sup>, (ii) monomeric cage [Pd<sub>2</sub>L<sup>2a</sup>]<sub>4</sub>(BF<sub>4</sub>)<sub>4</sub>, and (iii) dimeric cage [Cl@Pd<sub>4</sub>L<sup>2a</sup>]<sub>8</sub>(BF<sub>4</sub>)<sub>7</sub> (400 MHz, 298 K, CD<sub>3</sub>CN). (b–d) ESI-FTICR mass spectra of (b) monomeric cage [Pd<sub>2</sub>L<sup>2a</sup>]<sub>4</sub>(BF<sub>4</sub>)<sub>4</sub>, (c) double cage [2BF<sub>4</sub>+Cl@Pd<sub>4</sub>L<sup>2a</sup>]<sub>8</sub>(BF<sub>4</sub>)<sub>5</sub>, and (d) the host–guest complex [2ReO<sub>4</sub>+Cl@Pd<sub>4</sub>L<sup>2a</sup>]<sub>8</sub>(BF<sub>4</sub>)<sub>5</sub>.

[Pd<sub>2</sub>L<sup>2a</sup>]<sub>4</sub>]<sup>4+</sup>, [Pd<sub>2</sub>L<sup>2a</sup>]<sub>4</sub>+BF<sub>4</sub>]<sub>3</sub>]<sup>3+</sup>, and [Pd<sub>2</sub>L<sup>2a</sup>]<sub>4</sub>+2BF<sub>4</sub>]<sub>2</sub>]<sup>2+</sup> in the high-resolution electrospray ionization Fourier transform ion cyclotron resonance (HR-ESI-FTICR) mass spectrum (Figure 2b).<sup>15</sup> Comparison of the calculated relative energies of the four possible stereoisomers further supported the formation of a single isomer in which all of the aryl substituents exhibit the same rotational sense [see the Supporting Information (SI)].

Interestingly, this monomeric cage species is thermodynamically stable without showing any signs of interpenetration in the presence of BF<sub>4</sub><sup>−</sup> anions in acetonitrile solution, in stark contrast to the monomeric [Pd<sub>2</sub>L<sup>1</sup>]<sub>4</sub> species formed by the

parent ligand L<sup>1</sup>, which is just a kinetic intermediate on the way to the thermodynamic end product [BF<sub>4</sub>@Pd<sub>4</sub>L<sup>1</sup>]<sub>8</sub>.<sup>12</sup> We attribute this behavior to the steric influence of the attached side arms of L<sup>2</sup>, which would clash with the other interpenetrating unit in a hypothetical [BF<sub>4</sub>@Pd<sub>4</sub>L<sup>2</sup>]<sub>8</sub> species.

Interpenetration of two {Pd<sub>2</sub>L<sup>2</sup>} units could, however, be enforced when 0.5 equiv of chloride was added to the solution containing monomeric cage [Pd<sub>2</sub>L<sup>2</sup>]<sub>4</sub> (Figure 1b). In this case, warming of the mixture led to a gradual transition into a solution in which the interpenetrated double cage [Cl@Pd<sub>4</sub>L<sup>2</sup>]<sub>8</sub> was the most abundant species, although it was obviously in equilibrium with minor amounts of [Pd<sub>2</sub>L<sup>2</sup>]<sub>4</sub> and free ligand L<sup>2</sup> (when F<sup>−</sup> or Br<sup>−</sup> was added as the template instead of Cl<sup>−</sup>, double cages were also formed, but in lower relative amounts). In full agreement with the findings for the double cage [BF<sub>4</sub>@Pd<sub>4</sub>L<sup>2a</sup>]<sub>8</sub>, the <sup>1</sup>H NMR spectrum of [Cl@Pd<sub>4</sub>L<sup>2a</sup>]<sub>8</sub> showed the typical pattern for an interpenetrated dimer with a twofold splitting of each signal and a pronounced downfield shift of the signals for the protons next to the pyridine N atoms, especially for the g' protons pointing into the central cavity [Figure 2a(iii)]. Furthermore, the most intense signals in the HR-ESI-FTICR mass spectrum can be assigned to the species [2BF<sub>4</sub>+Cl@Pd<sub>4</sub>L<sup>2a</sup>]<sub>8</sub>]<sup>5+</sup> and [2BF<sub>4</sub>+Cl@Pd<sub>4</sub>L<sup>2a</sup>]<sub>8</sub>+BF<sub>4</sub>]<sub>4</sub>]<sup>4+</sup>, in which the central pocket contains one chloride anion and each of the two outer pockets is filled with a BF<sub>4</sub><sup>−</sup> anion (Figure 2c). In addition, we were able to obtain single crystals of [Cl@Pd<sub>4</sub>L<sup>2b</sup>]<sub>8</sub> suitable for X-ray analysis by slow evaporation of a solution in acetonitrile. Figure 3 compares the structures of the previously reported BF<sub>4</sub><sup>−</sup>-templated double cage [BF<sub>4</sub>@Pd<sub>4</sub>L<sup>1</sup>]<sub>8</sub> (Figure 3a, left)<sup>12</sup> and the Cl<sup>−</sup>-templated double cage [Cl@Pd<sub>4</sub>L<sup>2b</sup>]<sub>8</sub> (Figure 3a, right) with respect to the Pd–Pd distance, the size of the templating anion, and the volume of the outer two pockets available for guest binding. Whereas the distance between the inner Pd centers decreases from 8.25 to 6.26 Å in going from the BF<sub>4</sub><sup>−</sup>-templated to the Cl<sup>−</sup>-templated double cage, the distance between an outer Pd and the nearer inner Pd increases from 8.09 to 8.79 Å. This change is also reflected in the volumes observed for the inner and outer pockets (Table 1).

We can explain the structural differences between [BF<sub>4</sub>@Pd<sub>4</sub>L<sup>1</sup>]<sub>8</sub> and [Cl@Pd<sub>4</sub>L<sup>2</sup>]<sub>8</sub> in terms of the cooperation of two factors: in L<sup>2</sup>, the introduction of steric bulk prevents the formation of a BF<sub>4</sub><sup>−</sup>-templated double cage. Hence, only a small anion such as chloride can template the dimerization, even in the presence of excess BF<sub>4</sub><sup>−</sup>, since it allows the aryl substituents of L<sup>2</sup> to steer clear of the ligand arms of the interpenetrating cage fragment (Figure 3b,c). This results in the formation of a small central cavity and two large outer pockets (visualized in Figure 3a by depicting the results of VOIDOO<sup>16</sup> cavity calculations).

Next, we examined the anion-binding capabilities of the double cage [Cl@Pd<sub>4</sub>L<sup>2</sup>]<sub>8</sub>. As expected, the selectivity of the outer pockets shifted toward larger guests. Whereas [BF<sub>4</sub>@Pd<sub>4</sub>L<sup>1</sup>]<sub>8</sub> was found to be a strong binder of halide anions (especially chloride), [Cl@Pd<sub>4</sub>L<sup>2</sup>]<sub>8</sub> showed a preference for the binding of larger anions such as perchlorate, hexafluorophosphate, and in particular perrhenate (see the SI). Figure 4a shows the results of the <sup>1</sup>H NMR titration of a CD<sub>3</sub>CN solution of [Cl@Pd<sub>4</sub>L<sup>2a</sup>]<sub>8</sub>(BF<sub>4</sub>)<sub>7</sub> with NBu<sub>4</sub>ReO<sub>4</sub>. In particular, protons a, g, and f', all of which point into the outer pockets, display downfield shifts upon ReO<sub>4</sub><sup>−</sup>-binding. In contrast, protons g' and a', which are close to the encapsulated chloride anion, are shifted upfield, most likely because the inner cavity

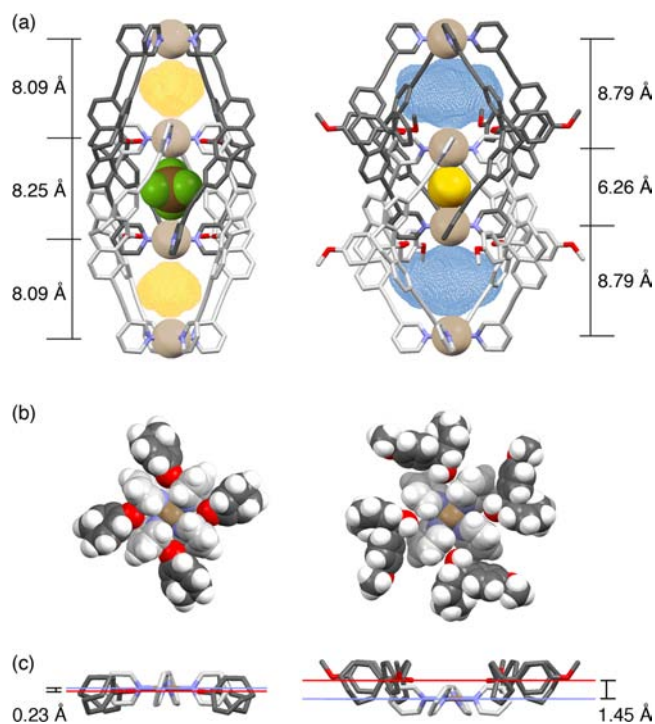


**Figure 3.** (a) Comparison of the X-ray structures of  $[\text{BF}_4@ \text{Pd}_4\text{L}^1_8](\text{BF}_4)_7$  (left)<sup>12</sup> and  $[\text{Cl}@ \text{Pd}_4\text{L}^{2b}_8](\text{BF}_4)_7$  (right). Color scheme: C, light/dark gray; N, blue; O, red; Cl, yellow; F, green; B, brown; Pd, beige. For clarity, H atoms, solvent molecules, and anions not in the central pockets have been omitted. (b) Space-filling top views and (c) stick side views of the inner  $\text{Pd}(\text{py})_4$  planes (H atoms omitted) illustrating the differences in the relative positions of the interpenetrating cage fragments in  $[\text{BF}_4@ \text{Pd}_4\text{L}^1_8](\text{BF}_4)_7$  (left) and  $[\text{Cl}@ \text{Pd}_4\text{L}^{2b}_8](\text{BF}_4)_7$  (right). In (c), the distances between the  $\text{N}_4$  and  $\text{O}_4$  planes are given.

**Table 1. Pocket Volumes and Packing Coefficients<sup>a</sup>**

	pocket	$[\text{BF}_4@ \text{Pd}_4\text{L}^1_8]^b$	$[\text{Cl}@ \text{Pd}_4\text{L}^{2b}_8]$
before guest addition	outer	49.9 ( $\text{BF}_4^-$ : 103%)	183.7 ( $\text{BF}_4^-$ : 28%)
	inner	108.9 ( $\text{BF}_4^-$ : 47%)	16.2 ( $\text{Cl}^-$ : 139%)
after guest addition	outer	23.5 ( $\text{Cl}^-$ : 96%)	183.7 ( $\text{ReO}_4^-$ : 35%) <sup>c</sup>
	inner	155.4 ( $\text{BF}_4^-$ : 33%)	16.2 ( $\text{Cl}^-$ : 139%) <sup>c</sup>

<sup>a</sup>Pocket volumes in  $\text{Å}^3$  and (guests: packing coefficients) of  $[\text{BF}_4@ \text{Pd}_4\text{L}^1_8]$  and  $[\text{Cl}@ \text{Pd}_4\text{L}^{2b}_8]$  before and after guest addition are shown. <sup>b</sup>Data from ref 13. <sup>c</sup>Based on the host structure before guest addition.

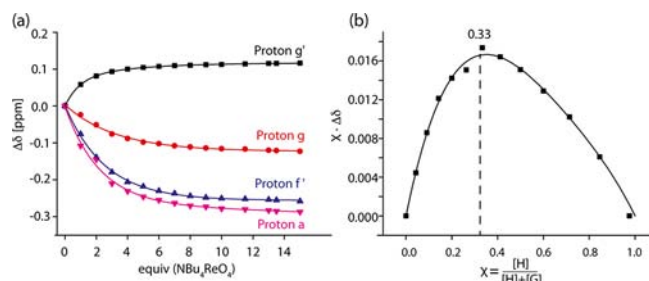


**Figure 4.** (a) Plot of  $^1\text{H}$  NMR signal shifts observed in the titration of  $[\text{Cl}@ \text{Pd}_4\text{L}^{2a}_8](\text{BF}_4)_7$  with  $\text{NBu}_4\text{ReO}_4$  ( $\text{CD}_3\text{CN}$ , 293 K). (b) Job plot analysis showing a  $\text{ReO}_4^- : [\text{Cl}@ \text{Pd}_4\text{L}^{2a}_8]$  ratio of 2:1.

slightly relaxes upon binding of  $\text{ReO}_4^-$  inside the outer pockets. Nonlinear data fitting<sup>17</sup> delivered the values  $K_1 = 2158 \pm 61 \text{ M}^{-1}$  and  $K_2 = 1848 \pm 30 \text{ M}^{-1}$  for binding of the first and

second guests, respectively. The fact that  $K_2$  is 3.4 times larger than the statistically expected value of  $K_1/4$  indicates positive cooperativity of the system. Furthermore, the 2:1 guest: host ratio was supported by Job plot analysis (Figure 4b) and the HR-ESI-FTICR mass spectrum of  $[2\text{ReO}_4 + \text{Cl}@ \text{Pd}_4\text{L}^{2a}_8](\text{BF}_4)_5$  (Figure 2d).

The observation that the strongly bound guest  $\text{Cl}^-$  in  $[2\text{Cl} + \text{BF}_4@ \text{Pd}_4\text{L}^1_8]$  showed slow exchange in the NMR experiments while the weakly bound guest  $\text{ReO}_4^-$  in  $[2\text{ReO}_4 + \text{Cl}@ \text{Pd}_4\text{L}^2_8]$  showed fast exchange kinetics is worth discussing. A plausible explanation can be given on the basis that the energy difference between the starting materials in the two processes is much smaller than the energy difference between the products of the guest encapsulation. This leads to a large difference in the  $\Delta G^\circ$  values for the two reactions and hence a large difference in the  $K$  values. If it is assumed that the rate constants for binding (the on rates) are comparable for the two processes, the difference in exchange kinetics is dominated by the rate constant for anion release from the pockets (the off rates), which is much smaller for  $\text{Cl}^-$  than for  $\text{ReO}_4^-$ .

To compare the anion selectivities, we performed cross experiments: when  $\text{Cl}^-$  was titrated into a solution of  $[\text{Cl}@ \text{Pd}_4\text{L}^{2a}_8]$ , a release of free ligand  $\text{L}^{2a}$  was observed in the  $^1\text{H}$  NMR spectrum instead of a shift in the proton signals of the double cage. This behavior was also observed when excess  $\text{Cl}^-$  was added to the chloride-saturated host-guest complex  $[2\text{Cl} + \text{BF}_4@ \text{Pd}_4\text{L}^1_8]$ .<sup>12</sup>

The outcome of the addition of  $\text{ReO}_4^-$  to  $[\text{BF}_4@ \text{Pd}_4\text{L}^1_8]$  was unexpected. Although shifts in some of the proton signals were observed in the  $^1\text{H}$  NMR titration, a binding constant could not be calculated in this case because mass spectrometric monitoring of the titration showed the partial formation of the species  $[3\text{ReO}_4@ \text{Pd}_4\text{L}^1_8]$  encapsulating a  $\text{ReO}_4^-$  anion instead of  $\text{BF}_4^-$  in the central pocket. We attribute this process to the better match of the size of a  $\text{ReO}_4^-$  anion with the volume of the inner cavity (packing coefficient of 58% for  $\text{ReO}_4^-$  vs 47% for  $\text{BF}_4^-$ ). Interestingly, the equilibrium between the  $\text{BF}_4^-$ - and  $\text{ReO}_4^-$ -templated double cages shifted toward the latter compound upon addition of chloride. This observation demonstrates the possibility of further extending the range of anionic templates in the central cavity.

Herein we have shown that the interpenetration and guest-binding abilities of dimeric coordination cages can be controlled by ligand derivatization and the choice of the templating anion. In contrast to our previous findings,<sup>12</sup> the introduction of bulky substituents into the ligand backbone allowed us to isolate monomeric cage species and induce dimerization by addition of the template at a later time. We have further shown that the size of the template inside the central pocket controls the size selectivity of allosteric anion binding in the two outer pockets. We think that our observations add to the understanding of anion-binding processes in dynamic supramolecular and biological systems. Furthermore, this strategy might find application in adaptive sensors and selective anion cotransporter systems.

## ■ ASSOCIATED CONTENT

### 📄 Supporting Information

Synthetic procedures; analytical data for  $\text{L}^{2a-c}$ ,  $[\text{Pd}_2\text{L}^{2a-c}_4](\text{BF}_4)_4$ , and  $[\text{Cl}@ \text{Pd}_4\text{L}^{2a-c}_8](\text{BF}_4)_7$ ; and NMR titration, ESI-MS, molecular modeling, and X-ray data. This material is available free of charge via the Internet at <http://pubs.acs.org>.



## ■ AUTHOR INFORMATION

## Corresponding Author

gclever@gwdg.de

## Notes

The authors declare no competing financial interest.

## ■ ACKNOWLEDGMENTS

This work was supported by the DFG through Grant CL 489/2-1 and the Fonds der Chemischen Industrie. We thank David M. Engelhard for the VOIDOO calculations.

## ■ REFERENCES

- (1) Palmer, L.; Rebek, J., Jr. *Org. Biomol. Chem.* **2004**, *2*, 3051.
- (2) Reviews: (a) Pluth, M. D.; Raymond, K. N. *Chem. Soc. Rev.* **2007**, *36*, 161. (b) Dalgarno, S. J.; Power, N. P.; Atwood, J. L. *Coord. Chem. Rev.* **2008**, *252*, 825. (c) Tranchemontagne, D. J.; Ni, Z.; O'Keeffe, M.; Yaghi, O. M. *Angew. Chem., Int. Ed.* **2008**, *47*, 5136. (d) Chakrabarty, R.; Mukherjee, P. S.; Stang, P. J. *Chem. Rev.* **2011**, *111*, 6810. (e) Ronson, T. K.; Zarra, S.; Black, S. P.; Nitschke, J. R. *Chem. Commun.* **2013**, *49*, 2476. (f) Cook, T. R.; Zheng, Y.-R.; Stang, P. J. *Chem. Rev.* **2013**, *113*, 734.
- (3) Further recent examples of self-assembled coordination cages: (a) Sun, Q. F.; Iwasa, J.; Ogawa, D.; Ishido, Y.; Sato, S.; Ozeki, T.; Sei, Y.; Yamaguchi, K.; Fujita, M. *Science* **2010**, *328*, 1144. (b) Sun, Q.-F.; Murase, T.; Sato, S.; Fujita, M. *Angew. Chem., Int. Ed.* **2011**, *50*, 10318. (c) Zheng, Y.-R.; Lan, W.-J.; Wang, M.; Cook, T. R.; Stang, P. J. *J. Am. Chem. Soc.* **2011**, *133*, 17045. (d) Turega, S.; Whitehead, M.; Hall, B. R.; Haddow, M. F.; Hunter, C. A.; Ward, M. D. *Chem. Commun.* **2012**, *48*, 2752. (e) Chepelin, O.; Ujma, J.; Barran, P. E.; Lusby, P. J. *Angew. Chem., Int. Ed.* **2012**, *124*, 4270. (f) Bivaud, S.; Balandier, J.-Y.; Chas, M.; Allain, M.; Goeb, S.; Sallé, M. *J. Am. Chem. Soc.* **2012**, *134*, 11968. (g) Riddell, I. A.; Smulders, M. M. J.; Clegg, J. K.; Hristova, Y. R.; Breiner, B.; Thoburn, J. D.; Nitschke, J. R. *Nat. Chem.* **2012**, *4*, 751. (h) Pasquale, S.; Sattin, S.; Escudero-Adán, E. C.; Martínez-Belmonte, M.; de Mendoza, J. *Nat. Commun.* **2012**, *3*, 785.
- (4) (a) Sessler, J. L.; Gale, P. A.; Cho, W.-S. *Anion Receptor Chemistry*; RSC Publishing: Cambridge, U.K., 2006. (b) Custelcean, R.; Bosano, J.; Bonnesen, P. V.; Kertesz, V.; Hay, B. P. *Angew. Chem., Int. Ed.* **2009**, *48*, 4025. (c) Thomas, J. A. *Dalton Trans.* **2011**, *40*, 12005. (d) Ma, Z.; Moulton, B. *Coord. Chem. Rev.* **2011**, *255*, 1623.
- (5) Clever, G. H.; Kawamura, W.; Tashiro, S.; Shiro, M.; Shionoya, M. *Angew. Chem., Int. Ed.* **2012**, *51*, 2606.
- (6) Clever, G. H.; Tashiro, S.; Shionoya, M. *J. Am. Chem. Soc.* **2010**, *132*, 9973.
- (7) Clever, G. H.; Kawamura, W.; Shionoya, M. *Inorg. Chem.* **2011**, *50*, 4689.
- (8) Clever, G. H. In *Molecules at Work*; Pignataro, B., Ed.; Wiley-VCH: Weinheim, Germany, 2012.
- (9) Han, M.; Michel, R.; He, B.; Chen, Y.-S.; Stalke, D.; John, M.; Clever, G. H. *Angew. Chem., Int. Ed.* **2013**, *52*, 1319.
- (10) Other examples of interpenetrated coordination cages: (a) Fujita, M.; Fujita, N.; Ogura, K.; Yamaguchi, K. *Nature* **1999**, *400*, 52. (b) Yamauchi, Y.; Yoshizawa, M.; Fujita, M. *J. Am. Chem. Soc.* **2008**, *130*, 5832. (c) Fukuda, M.; Sekiya, R.; Kuroda, R. *Angew. Chem., Int. Ed.* **2008**, *47*, 706. (d) Westcott, A.; Fisher, J.; Harding, L. P.; Rizkallah, P.; Hardie, M. J. *J. Am. Chem. Soc.* **2008**, *130*, 2950. (e) Heine, J.; Schmedt auf der Günne, J.; Dehnen, S. *J. Am. Chem. Soc.* **2011**, *133*, 10018. (f) Sekiya, R.; Fukuda, M.; Kuroda, R. *J. Am. Chem. Soc.* **2012**, *134*, 10987.
- (11) Charges and counteranions have been partially omitted in formulas for simplicity.
- (12) Freye, S.; Hey, J.; Torras-Galán, A.; Stalke, D.; Herbst-Irmer, R.; John, M.; Clever, G. H. *Angew. Chem., Int. Ed.* **2012**, *51*, 2191.
- (13) Freye, S.; Engelhard, D. M.; John, M.; Clever, G. H. *Chem.—Eur. J.* **2013**, *19*, 2114.
- (14) Dieterich, J. M.; Clever, G. H.; Mata, R. A. *Phys. Chem. Chem. Phys.* **2012**, *14*, 12746.
- (15) Examples of other  $[M_2L_4]$  cages: (a) McMorran, D.; Steel, P. *Angew. Chem., Int. Ed.* **1998**, *37*, 3295. (b) Chand, D. K.; Biradha, K.; Fujita, M. *Chem. Commun.* **2001**, 1652. (c) Su, C.; Cai, Y. P.; Chen, C.; Smith, M. D.; Kaim, W.; zur Loye, H. C. *J. Am. Chem. Soc.* **2003**, *125*, 8595. (d) Yue, N. L. S.; Eisler, D. J.; Jennings, M. C.; Puddephatt, R. J. *Inorg. Chem.* **2004**, *43*, 7671. (e) Clever, G. H.; Tashiro, S.; Shionoya, M. *Angew. Chem., Int. Ed.* **2009**, *48*, 7010. (f) Liao, P.; Langloss, B. W.; Johnson, A. M.; Knudsen, E. R.; Tham, F. S.; Julian, R. R.; Hooley, R. J. *Chem. Commun.* **2010**, *46*, 4932. (g) Kishi, N.; Li, Z.; Yoza, K.; Akita, M.; Yoshizawa, M. *J. Am. Chem. Soc.* **2011**, *133*, 11438. (h) Lewis, J. E. M.; Gavey, E. L.; Cameron, S. A.; Crowley, J. D. *Chem. Sci.* **2012**, *3*, 778.
- (16) Kleywegt, G. J.; Jones, T. A. *Acta Crystallogr., Sect. D* **1994**, *50*, 178.
- (17) Thordarson, P. *Chem. Soc. Rev.* **2011**, *40*, 1305.